

Multilayer Optics for an Extreme Ultraviolet Lithography Tool with 70 nm Resolution

R. Soufli, E. Spiller, M. A. Schmidt, J. C. Davidson, R. F. Grabner, E. M. Gullikson, B. B. Kaufmann, S. L. Baker, H. N. Chapman, R. M. Hudyma, J. S. Taylor, C. C. Walton, C. Montcalm, J. A. Folta

*This article was submitted to
Society for Photo-Optical Instrumentation Engineers 26th
International Symposium Emerging Lithographic Technologies V
Santa Clara, CA
February 26 – March 2, 2001*

U.S. Department of Energy

Lawrence
Livermore
National
Laboratory

May 4, 2001

DISCLAIMER

This document was prepared as an account of work sponsored by an agency of the United States Government. Neither the United States Government nor the University of California nor any of their employees, makes any warranty, express or implied, or assumes any legal liability or responsibility for the accuracy, completeness, or usefulness of any information, apparatus, product, or process disclosed, or represents that its use would not infringe privately owned rights. Reference herein to any specific commercial product, process, or service by trade name, trademark, manufacturer, or otherwise, does not necessarily constitute or imply its endorsement, recommendation, or favoring by the United States Government or the University of California. The views and opinions of authors expressed herein do not necessarily state or reflect those of the United States Government or the University of California, and shall not be used for advertising or product endorsement purposes.

This is a preprint of a paper intended for publication in a journal or proceedings. Since changes may be made before publication, this preprint is made available with the understanding that it will not be cited or reproduced without the permission of the author.

This report has been reproduced directly from the best available copy.

Available electronically at <http://www.doc.gov/bridge>

Available for a processing fee to U.S. Department of Energy
And its contractors in paper from
U.S. Department of Energy
Office of Scientific and Technical Information
P.O. Box 62
Oak Ridge, TN 37831-0062
Telephone: (865) 576-8401
Facsimile: (865) 576-5728
E-mail: reports@adonis.osti.gov

Available for the sale to the public from
U.S. Department of Commerce
National Technical Information Service
5285 Port Royal Road
Springfield, VA 22161
Telephone: (800) 553-6847
Facsimile: (703) 605-6900
E-mail: orders@ntis.fedworld.gov
Online ordering: <http://www.ntis.gov/ordering.htm>

OR

Lawrence Livermore National Laboratory
Technical Information Department's Digital Library
<http://www.llnl.gov/tid/Library.html>

Multilayer optics for an extreme ultraviolet lithography tool with 70 nm resolution

Regina Soufli^{*a}, Eberhard Spiller^a, Mark A. Schmidt^a, J. Courtney Davidson^a, R. Frederick Grabner^a, Eric M. Gullikson^b, Benjamin B. Kaufmann^a, Sherry L. Baker^a, Henry N. Chapman^a, Russell M. Hudyma^a, John S. Taylor^a, Christopher C. Walton^a, Claude Montcalm^a, James A. Folta^a

^aLawrence Livermore National Laboratory, 7000 East Avenue, Livermore, CA 94550

^bLawrence Berkeley National Laboratory, 1 Cyclotron Road, Berkeley, CA 94720

ABSTRACT

One of the most critical tasks in the development of extreme ultraviolet lithography (EUVL) is the accurate deposition of reflective multilayer coatings for the mirrors comprising the EUVL tool. The second set (Set 2) of four imaging optics for an alpha-class EUVL system has been coated successfully. All four mirrors (M1, M2, M3, M4) were Mo/Si-coated during a single deposition run with a production-scale DC-magnetron sputtering system. Ideally, the multilayer coatings should not degrade the residual wavefront error of the imaging system design. For the present EUVL camera, this requirement is equivalent to depositing multilayer coatings that would add a figure error of less than 0.11 nm rms. In addition, all mirrors should be matched in centroid wavelength, in order to insure maximum throughput of the EUVL tool. In order to meet these constraints, the multilayer deposition process needs to be controlled to atomic precision. EUV measurements of the coated mirrors determined that the added figure errors due to the multilayer coatings are 0.032 nm rms (M1), 0.037 nm rms (M2), 0.040 nm rms (M3) and 0.015 nm rms (M4), well within the aforementioned requirement of 0.11 nm rms. The average wavelength among the four projection mirrors is 13.352 nm, with an optic-to-optic matching of $1\sigma=0.010$ nm. This outstanding level of wavelength matching produces 99.3% of the throughput of an ideally matched four-mirror system. Peak reflectances are 63.8% (M1), 65.2% (M2), 63.8% (M3) and 66.7% (M4). The variation in reflectance values between the four optics is consistent with their high frequency substrate roughness. It is predicted that the multilayer coatings will not introduce any aberrations in the lithographic system performance, for both static and scanned images of 70 nm –dense features.

Keywords: Multilayer optics, reflectivity, thickness uniformity, extreme ultraviolet (EUV) lithography

1. INTRODUCTION

Highly reflective, atomic-precision multilayer coatings have been the enabling technology for the development of extreme ultraviolet lithography (EUVL) as the leading next-generation lithography candidate. Today, it is believed that EUVL will be first implemented for high volume manufacturing to print features at –or below- 70 nm and will have the potential of extendibility down to the 30-nm node^{1,2}. EUVL tools are based on all-reflective system designs: they use multilayer mirrors for their illumination and projection systems, and have a multilayer-coated reflective mask. The Engineering Test Stand (ETS) is a prototype laboratory system currently operating at a wavelength of 13.4 nm, developed to demonstrate full-field printing of EUV images and is described in References 3, 4. The ETS camera has a 4x-reduction, ring field design with a numerical aperture of 0.1 and consists of four curved multilayer mirrors. Two sets of substrates have been manufactured and multilayer-coated for the ETS projection system. The first set (Set 1) is a developmental set of optics, designed to demonstrate printing of features down to the 100 nm size. The Set 1 projection mirrors are currently installed in the ETS and have successfully produced 100-nm resolution images^{3,4,5}. The second –and final- set of projection optics for the ETS (Set 2) was designed with tighter substrate figure, finish and multilayer thickness specifications. The purpose of the Set 2 optics is to produce images of 70 nm-dense features. This manuscript discusses the coating and characterization of the four Set 2 multilayer mirrors for the ETS camera.

* E-mail correspondence: soufli1@llnl.gov; phone (925) 422 6013; fax (925) 423 1488

2. MULTILAYER COATING REQUIREMENTS FOR THE ETS AND BEYOND

All multilayer coatings for the ETS projection system are required by the optical design to be uniform across the optic surface. There are several criteria that need to be satisfied when specifying thickness tolerances for multilayer-coated optics for lithography applications⁶. All specifications given below apply to the illuminated area of each mirror surface (clear aperture area) in the ETS camera. The clear aperture is defined for each ETS optic in Table 1.

2.1 Throughput considerations

The ETS is an all-reflective system with multilayer coatings on four projection elements, two condenser assemblies of six elements each, and on the mask. All of these elements should be tuned to reflect at –or near- the same wavelength λ , in order to obtain a substantial output signal from the camera. For a commercial EUVL tool, a spectral mismatch between the mirrors would translate to throughput reduction. Originally, a goal was set to match the reflectance peak position of all ETS optics to within $\Delta\lambda = \pm 0.055$ nm, which would ensure at least 85% of system throughput compared to the ideal wavelength-matching case⁵. Meeting this goal requires atomic-level repeatability of the coating process from one deposition run to another. In addition to optic-to-optic wavelength matching, another throughput constraint is the tolerance on wavelength variation across the surface of any individual optic in the system. For maximum throughput, the multilayer should have its reflectivity peak at the same wavelength for all surface points on any given mirror. If an arbitrary goal is set for λ to stay within 99% of the reflectivity peak for all points on the optic surface, then a Mo/Si multilayer operating at $\lambda=13.4$ nm is allowed to have its wavelength vary to within $\Delta\lambda = \pm 0.05$ nm, which is equivalent to having the wavelength, or the thickness, vary to within $\pm 0.37\%$ peak-to-valley (P-V) across the surface.

2.2 Intensity variations

A reflectivity mismatch across any individual mirror surface in the projection system results in intensity variations (apodization) of the reflected wavefront at the system exit pupil. In lithography terms, this effect causes loss of aerial image contrast and variations in the critical dimension (CD) of scanned images across the field, thus degrading the imaging performance. The tolerance for this effect was determined to be $\pm 0.2\%$ P-V for wavelength (or thickness) uniformity across each of the four ETS Set 2 projection optics.

2.3 Figure errors

Wavefront errors due to multilayer thickness variations corresponding to long spatial frequencies (figure) introduce aberrations which are detrimental to the overall performance of the imaging system. Such multilayer-induced errors can be decomposed into a compensable and a non-compensable part. What remains after aligning-out the compensable part of the thickness error is the added (non-compensable) figure error that the multilayer is contributing to the system, as is explained in Section 4.1. In order for multilayer coatings to not affect adversely the imaging system performance, their added figure error should be negligible compared to the substrate figure error. For the Set 2 substrates, the specification for the figure error was 0.25 nm rms, as is shown in Table 2. The maximum allowable added figure error due to the Set 2 multilayer coatings was then set at 0.11 nm rms, which for a typical 280 nm-thick Mo/Si film corresponds to 0.04% rms (0.1% P-V).

2.4 Summary of coating tolerances for the Set 2 optics

The tightest among the constraints imposed to the multilayer thickness variation in Sections 2.1-2.3, are the $\pm 0.2\%$ P-V thickness uniformity and the 0.11 nm rms added figure error requirements. Both these specifications have to be met independently for a given multilayer coating: the $\pm 0.2\%$ P-V criterion is applied to the as-measured multilayer thickness profile, while the added figure error is determined from the non-compensable portion of the as-measured profile (see Section 4.1). Satisfying the 0.11 nm rms added figure error constraint depends to a large degree on the “shape” of the thickness profile, i.e. profile shapes approaching a 2nd order polynomial produce the lowest added figure errors. During the process of engineering the coating recipes for the four ETS Set 2 projection mirrors and testing various experimental profiles, it was concluded that the 0.11 nm rms added figure error tolerance requires the tightest control on the coating thickness. For this reason, the Set 2 thickness profiles presented in Section 4.1 are optimized for lowest added figure error, rather than P-V uniformity.

2.5 Future tool requirements

The next generation of EUVL projection optics will be implemented in beta and production tools. Substrate figure requirements have been set at about 0.1 nm rms for these systems. Consequently, multilayer-added figure errors of less than 0.05 nm rms should be achieved, a factor of 2 more stringent than the ETS camera requirements. Future tool designs include six-mirror cameras, with the clear aperture for some of these mirrors extending up to 200 mm from the optical axis. The

prescription for these elements may require graded coatings. In order to meet all these additional degrees of difficulty imposed on beta and production multilayer coatings, extremely sophisticated control of the multilayer film thickness would be required. The results presented in Section 4.1 are quite promising in this direction.

3. EXPERIMENTAL SETUP

		Clear Aperture		
		y₀ (mm)	y (mm)	x (mm)
M1	asphere, best-fit R _c = -3055 mm	114.9	± 25	± 56.2
M2	asphere, best-fit R _c = +1088 mm	103	± 49.6	± 78.1
M3	sphere, R _c = -389 mm	0	± 25.4	± 25.4
M4	asphere, best-fit R _c = +504 mm	52.8	± 45	± 59

Table 1: Geometry of the four ETS projection optics. M1, M2 and M4 are sections of aspheres, with a maximum departure of a few μm from a best-fit sphere, in the clear aperture area. M1 and M3 are convex (radius of curvature R_c is negative), while M2 and M4 are concave (R_c is positive). y₀ is the distance between the optical axis and the center of the clear aperture and y, x, define the extent of the clear aperture, measured from its center.

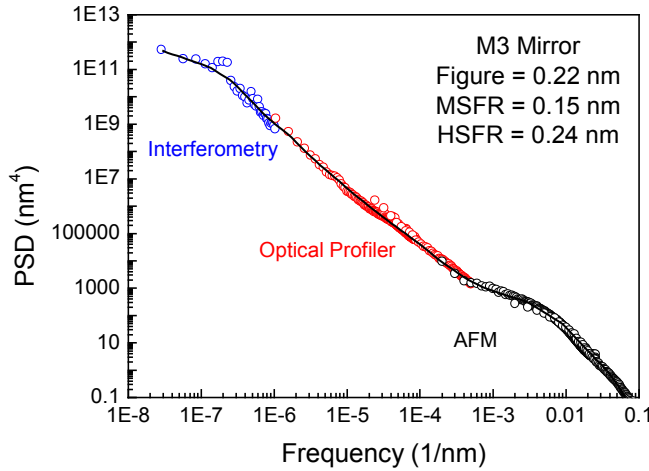


Figure 1: Measured PSD of the M3 substrate surface. For each spatial frequency range, the area under the PSD curve is used to determine the rms value of the roughness.

	Figure (nm rms)	MSFR (nm rms)	HSFR (nm rms)
M1	0.25	0.21	0.24
M2	0.35	0.20	0.19
M3	0.22	0.15	0.24
M4	0.25	0.22	0.17
Spec	0.25	0.20	0.10

Table 2: Summary of figure and finish results in the clear aperture area of the delivered ETS Set 2 optics, compared to the specifications.

3.1 Optical substrates

The four projection optics substrates were made of Zerodur™ and were polished by SVG-Tinsley (Richmond, California). Table 2 contains the measured values for the figure and finish of the delivered Set 2 substrates. Surface figure errors include contributions from long spatial scale height variations, resulting mostly in low-order aberrations of the imaging system. Mid-spatial frequency roughness (MSFR) includes the spatial period range 1 mm – 1 μm and contributes to flare in the imaging

system. High spatial frequency roughness (HSFR) corresponds to spatial periods below 1 μm , which are responsible for non-specular scattering leading in reduced reflectance of the multilayer-coated optics and ultimately in loss of throughput of the lithographic tool. Visible-light interferometry, optical profilometry and atomic force microscopy measurements on several locations on the surface were used in order to construct the two-dimensional power spectral density (PSD) for each optic (see Figure 1). Through the PSD, an rms value for the roughness in each spatial frequency range was determined. Table 2 summarizes these results for the four Set 2 substrates. Substrate figure requirements were met for M1, M3, and M4. A factor of 2 improvement in figure was achieved over the previously manufactured Set 1 substrates, expected to lead to enhanced resolution in the ETS performance with the Set 2 optics⁴. M2 underwent a figure deformation due to a machining operation and was accepted after it was verified that this type of deformation would not degrade the imaging performance of the ETS. MSFR values were improved for all Set 2 optics, compared to Set 1 optics⁴. On the other hand, the HSFR specification of 0.1 nm rms was not met for the Set 2 substrates, indicating a possible trade-off between the figuring and finishing processes. The values of HSFR are directly linked to the reflectance and scattering results from the multilayer-coated Set 2 mirrors, presented in Section 4 of this paper. The manufacturing and metrology of the ETS projection optics substrates are discussed in more detail in References 3, 4.

3.2 Multilayer deposition system

A newly acquired DC-magnetron sputtering system, shown in Figure 2, was used at LLNL in order to coat the four projection optics (M1, M2, M3, M4) of the ETS camera. This sputtering system was developed in partnership with Veeco Instruments, Inc. (Plainview, New York). It is a production-scale deposition tool, with a platter radius about 3 times larger than the platter radius of the laboratory tool that was used to coat the previous set (Set 1) of ETS projection optics⁵, as is demonstrated in Figure 3. The size of the new tool allows the coating of large optics (four optics of up to 470 mm in diameter can be accommodated in the deposition chamber) and the off-center mounting and spinning of optics with the possibility of graded coatings. The new tool has a “sputter down” geometry, shown in Figure 2 (left), with five sputtering targets available. Figure 3 shows a pair of targets, placed 180° apart, which are used during a typical Mo/Si deposition run. The Mo source is operated at a power of 1000 W and Si at 2500 W. The Ar process gas sputtering pressure is typically at 1 mTorr. During a multilayer

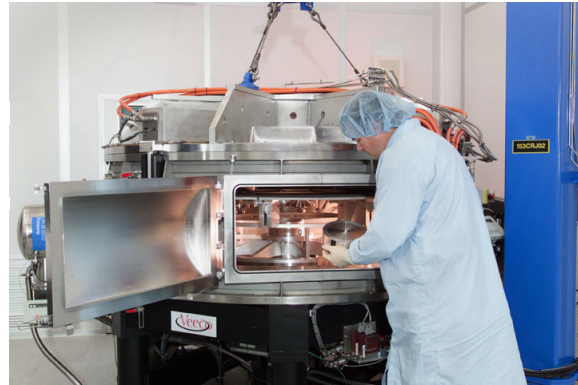
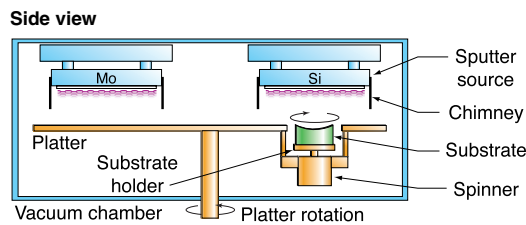


Figure 2: Side view of the DC-magnetron sputtering system used to coat the Set 2 projection optics. The diagram on the left shows the main components of the deposition chamber. The photograph on the right displays an optic being introduced into the chamber through a side door.

deposition run, the platter is rotating under the sources at a speed of about 1 rpm, while the individual substrates are simultaneously spinning around their centers, in order to average out spatial variations of the sputtering sources. The platter speed is modulated as each substrate passes under the Si and Mo targets, in order to achieve the desired multilayer thickness profile for each optic. Spinning velocities were set to 300 rpm (6 Hz) for the multilayer coatings discussed in this work.

Figure 3 (b) shows the deposition system configured to accommodate the ETS Set 2 imaging optics. The capacity of the deposition chamber allowed all four Set 2 optics to be coated during the same deposition run, insuring best optic-to-optic wavelength matching, as is going to be discussed in Section 4.1. The four Set 2 mirrors were spun around their optical axis and not around the center of their clear aperture, as was the case for the Set 1 coatings⁵. As is shown in Table 1, the optical

axis is outside the clear aperture area for mirrors M1, M2, M4 and coincides with the center of the clear aperture only for mirror M3. The advantage of the Set 2 coating geometry is that all thickness errors are rotationally symmetric around the optical axis and affect all field points in the same way, easing the task of compensating errors in the alignment of the ETS. On the other hand, multilayer thickness has to be controlled at larger radii with the Set 2 coating arrangement, thus, achievement of the desired thickness profile becomes more challenging.

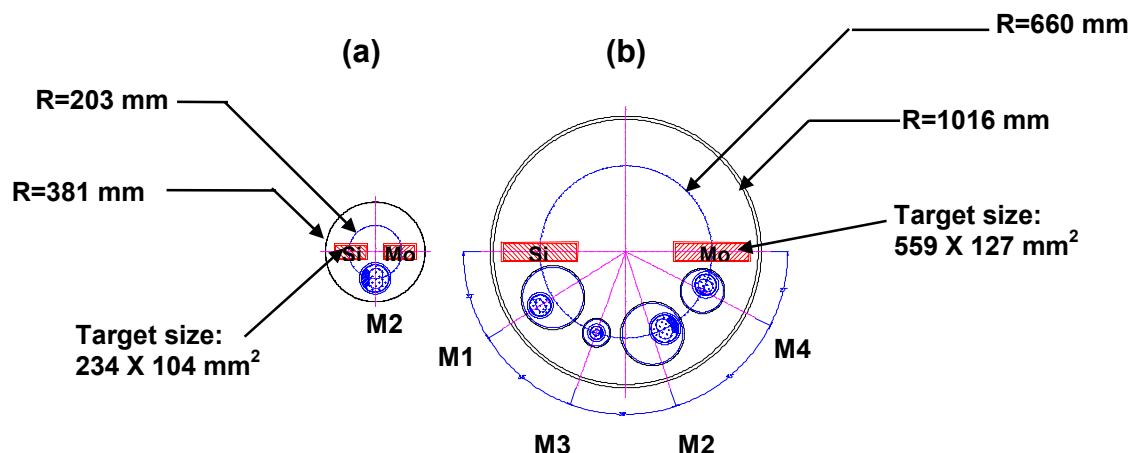


Figure 3: Top-view diagrams of the two deposition systems used to coat (a) the ETS Set 1 optics and (b) the ETS Set 2 optics.

3.3 EUV reflectance and scattering measurements

The EUV reflectance of the ETS Set 2 coatings was measured at beamline 6.3.2. of the Advanced Light Source synchrotron at Lawrence Berkeley National Laboratory. The characteristics of the beamline 6.3.2. reflectometer are described in detail in References 7, 8. Curved optics of up to 200 mm in diameter can be mapped in this facility. The reflectometer sample stage allows motion of an optic in 3 dimensions, tilt in 2 dimensions and azimuthal rotation of the sample holder. The detector arm can be rotated 360° around the axis of the reflectometer chamber. Once an optic is aligned, custom-designed software allows the operator to pre-calculate for each surface point a table of all coordinates of the sample stage, and program wavelength scans on multiple locations on the mirror surface without any manual input needed in-between scans. The reflectometer used a Si photodiode detector, with an acceptance angle of 2.4°. All wavelength and reflectance measurements were obtained with a 0.002 nm and 0.2% (absolute) precision, respectively[†]. The EUV reflectance results are discussed in Section 4.1. Off-specular EUV scattering was also measured for each of the four coated mirrors at the beamline 6.3.2. reflectometer. Scattered light was measured using a channel electron multiplier (CEM) with an acceptance angle of 0.24°. Up to 10 orders of dynamic range can be obtained with this instrument. In order to plot the scattering on an absolute scale, the incident intensity was measured with the Si photodiode and the efficiency of the CEM was measured relative to the photodiode using an intensity range where both detectors could be used. The detection efficiency of the CEM was thus determined to be about 5%. The scattering results are discussed in Section 4.2.

4. DISCUSSION OF RESULTS

4.1 Multilayer wavelength, thickness and reflectance results

EUV reflectance vs. wavelength curves were measured for several locations on each mirror surface. Measurements were performed at a fixed angle of incidence for each ETS mirror: 4° for M1, 6.55° for M2, 12° for M3 and 6° for M4 (all angles specified from normal incidence). The peak wavelength and reflectance were determined for each reflectance curve and the thickness profile for each multilayer coating was obtained from the measured values of wavelength, normalized at an arbitra-

[†] The beamline 6.3.2. reflectometer has been upgraded since these measurements were performed. It currently delivers precision of 0.001 nm for wavelength and 0.05% (absolute) for peak reflectance in the Mo/Si range. See also Reference 8 in these Proceedings.

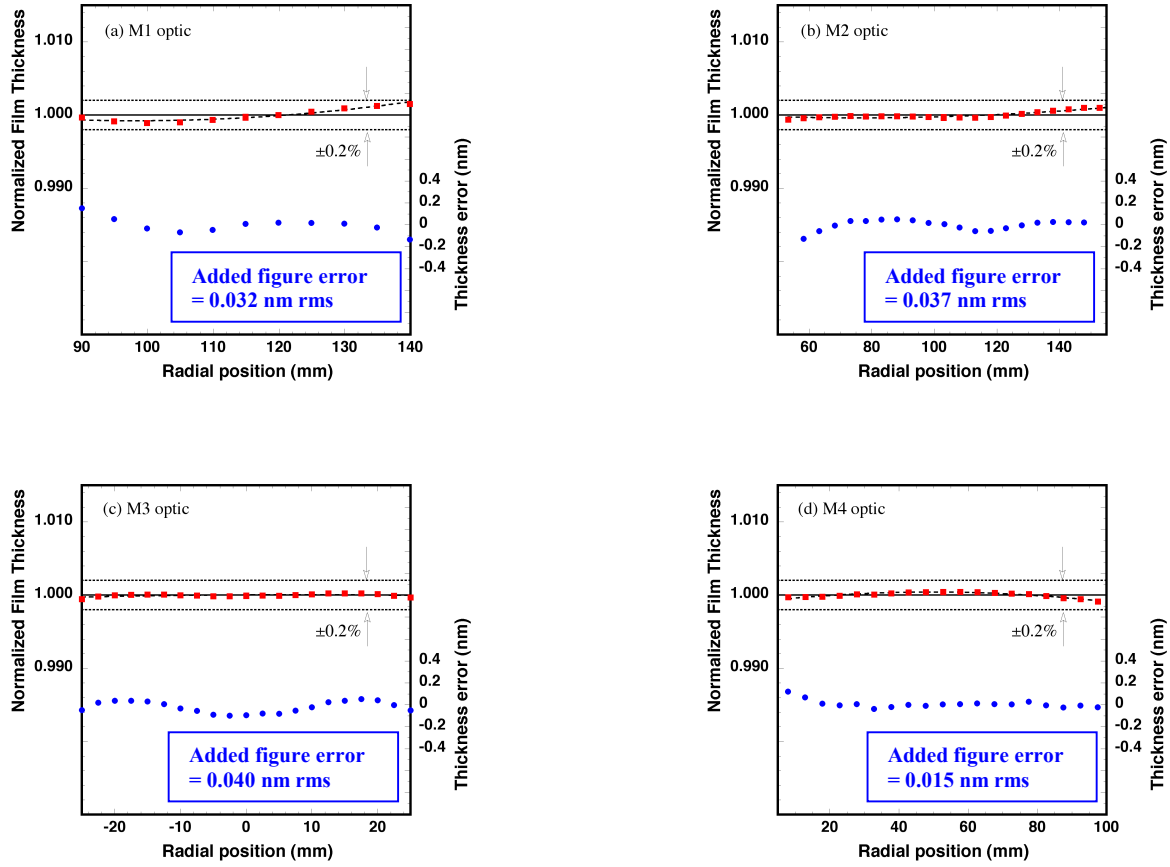


Figure 4: Measured thickness profile results are plotted vs. radial distance from the optical axis for the four ETS Set 2 mirrors. The clear aperture area of each optic is shown. In each plot, the top curve (left y-axis, unitless) is the normalized film thickness. All four coatings are well within the $\pm 0.2\%$ P-V uniformity requirement. The bottom curve (right y-axis, in nm) represents the un-compensable figure error that the multilayer stack is adding to the system. All four multilayer coatings are contributing added figure errors well below the 0.11 nm rms specification.

ry point on the optic surface. As is explained in Section 3.2, all mirrors were spun around their optical axis during multilayer deposition. Therefore, it is expected that the coatings should be uniform along circles centered at the optical axis (this fact was also verified experimentally and is discussed later in this Section). Figure 4 displays the normalized thickness profile results as a function of radial distance from the optical axis, for all four ETS Set 2 projection optics. The P-V thickness uniformity specification of $\pm 0.2\%$, discussed in Section 2, was met for all four coatings. A portion of the non-uniformity, represented by a linear and a spherical change in thickness across the optic surface, can be compensated during alignment of the system by performing rigid body motions and focus shifts of the mirrors. The added (non-compensable) figure error is what remains after subtraction of the compensable part from the measured thickness profile curve. This difference is plotted in Figure 4 as the thickness error (in nm) that a 280 nm multilayer film is contributing at each location on the optic surface. The standard deviation of this difference, weighted with the illuminated area corresponding to each radial point on the optic surface, is the rms added figure error that is given for each mirror in Figure 4. The coating strategy was to minimize this non-compensable component for all four mirrors. The added figure errors due to the multilayer coatings were thus determined to be 0.032 nm rms (M1), 0.037 nm rms (M2), 0.040 nm rms (M3) and 0.015 nm rms (M4), well within the requirement of 0.11 nm rms, discussed in Section 2. The peak wavelength of each optic, weighted across the clear aperture area, was found to be 13.355 nm (M1), 13.347 nm (M2), 13.363 nm (M3) and 13.342 nm (M4), resulting in an average wavelength of 13.352 nm for the projection optics system, with an optic-to- optic matching of $1\sigma=0.010$ nm. This level of wavelength matching yields

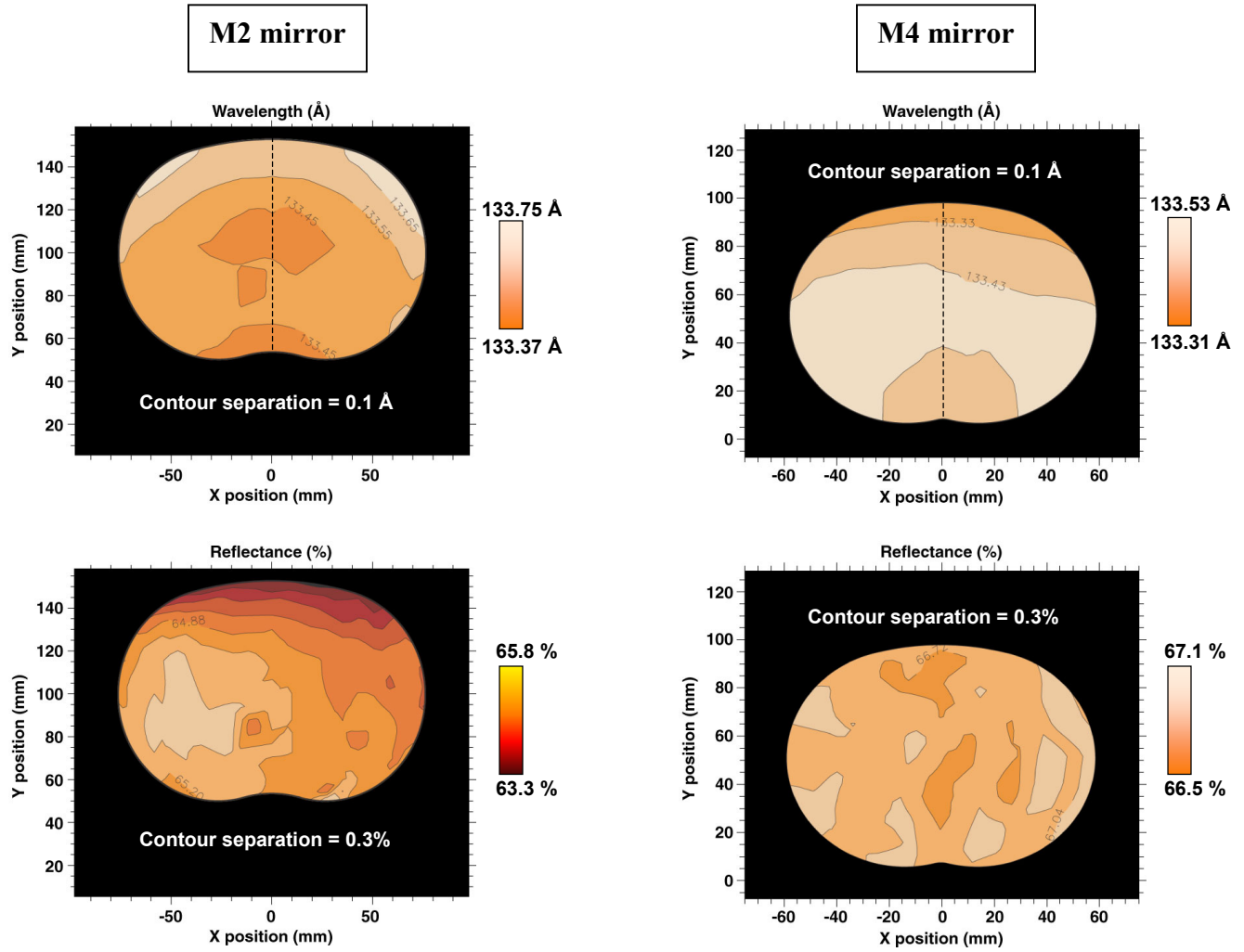


Figure 5: Two-dimensional contour maps of wavelength (top) and reflectance (bottom) in the clear aperture area of the M2 (left) and the M4 (right) mirrors. The wavelength maps confirm the multilayer thickness uniformity over the entire surface and the rotational symmetry of the coating process around the optical axis, located at (x,y)=(0,0) mm. The dashed line marks the location of the normalized thickness results for M2 and M4 plotted in Figure 4. A 2.5% variation in absolute reflectance across the M2 surface indicates that the M2 substrate has the least uniform finish among the four ETS Set 2 projection optics. On the other hand, M4 has the most uniform substrate finish with 0.6% variation in reflectance across the clear aperture area.

99.3% of the throughput of an ideally matched four-mirror system and is an improvement over the wavelength matching of $1\sigma=0.032$ nm (96% of throughput) achieved for the Set 1 optics⁵. The improvement is mostly due to the fact that all four Set 2 optics were coated during the same deposition run with the new DC-magnetron system, while the Set 1 optics had to be coated one-at-a-time, due to size limitations of the previous deposition system that was available, as shown in Figure 3. The outstanding levels of wavelength matching obtained for both Set 1 and Set 2 mirrors have by far exceeded the 85% throughput expectations set in Section 2.1 and thus have eliminated wavelength mismatch as a factor contributing to significant loss of throughput in the ETS system.

Peak reflectances were measured at 63.8% (M1), 65.2% (M2), 63.8% (M3) and 66.7% (M4) at the center of the clear aperture of each optic. The variation in reflectance values among the four optics is consistent with the rms high spatial frequency roughness values of their substrates, and was verified through atomic force microscopy characterization of the substrates prior to coating and scattering measurements of the coated optics. These results are discussed in Section 4.2 and summarized in Table 3.

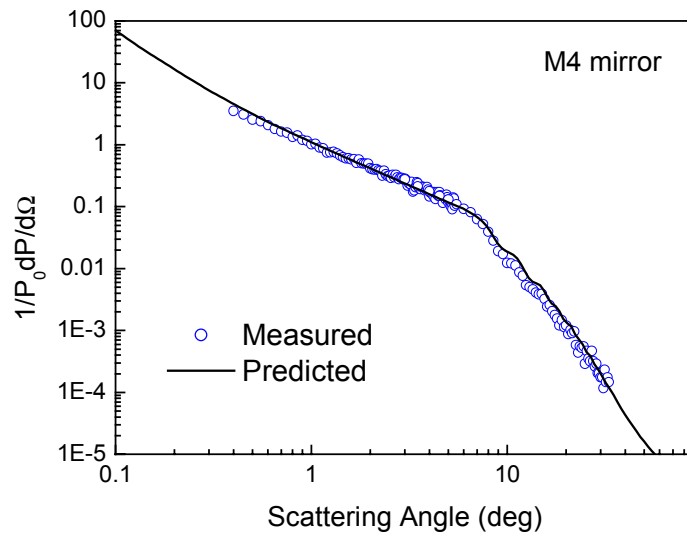


Figure 6: The angular distribution of light scattered from the M4 mirror. EUV light was incident at 6 degrees off normal. The predicted distribution was calculated using a dynamical scattering theory and the measured substrate PSD.

In addition to the radial direction shown in Figure 4, reflectance measurements were obtained in several other directions on each mirror surface, in order to construct two-dimensional contour maps of peak wavelength and reflectance, as shown in Figure 5. The wavelength information contained in the two-dimensional contour maps can also be derived from one-dimensional data such as those in Figure 4, using the rotational symmetry of the coatings around the optical axis; the wavelength contour maps just confirm this symmetry. The reflectance values, on the other hand, are strongly influenced by the high frequency roughness of the Zerodur substrates and therefore provide useful information about the substrate finish topography of each mirror. Reflectance variations across the surface of a multilayer-coated optic indicate varying levels of roughness on the underlying substrate (assuming that the wavelength remains uniform across the surface, as is the case for the ETS coatings). As an example, measured contour maps for mirrors M2 and M4 are shown in Figure 5. After producing contour maps for all four Set 2 mirrors, it was determined that reflectance varied within the clear aperture area by 0.7% (M1), 2.5% (M2), 1% (M3) and 0.6% (M4), all values absolute. These results are in agreement with atomic force microscopy measurements obtained on isolated points on each optic surface prior to coating. Reflectance variations across the illuminated area of a given optic are undesirable since they cause intensity variations (apodization) in the system exit pupil, which may degrade the performance of the imaging system. Simulations using the measured reflectance maps of the four ETS Set 2 mirrors predicted a <1% loss in contrast and a correctable CD variation of < 1 nm across the 24 mm image field, for 70-nm scanned lines. Thus, apodization effects due to varying substrate roughness in the ETS camera will be negligible. In the future, specifications will be set for the substrate finish uniformity of beta and production tool optics (in addition to the rms specifications), in order to prevent such problems in the lithographic performance of commercial systems.

4.2 EUV scattering results

The angular distribution of non-specularly scattered light was measured for each of the four coated mirrors. Measurements were performed at the nominal angle of incidence of each of the mirrors in the ETS camera, at the peak wavelength previously determined from the EUV reflectance measurements discussed in Section 4.1. Scattering results from the M4 mirror are shown in Figure 6. The experimental data are in excellent agreement with the predicted distribution. The predicted distribution was calculated with the distorted wave Born approximation⁹ using the measured PSD of the substrate. The effect of the multilayer was included using a linear growth model by Stearns¹⁰. For scattering angles below about 6 degrees the angular distribution is proportional to the PSD. For angles larger than 6 degrees the scattering drops off faster than the PSD since light scattered from the individual interfaces within the multilayer no longer adds in phase. The scattering was also measured for the other mirrors and good agreement was obtained with the predicted distribution. Angular scattering was integrated over all angles in two dimensions in order to obtain the total integrated scattering (TIS), expressed as loss in absolute reflectance. Table 3 gives a summary of these results. The difference in the amount of scattering between the four mirrors is caused by the difference in the HSFR values of the mirror substrates. All measured results are consistent with each other, meaning that the optics with the lowest substrate roughness exhibit the lowest amount of scattering and the highest peak reflectance values. The only exception is the TIS from mirror M3, where scattering appears somewhat lower than would be anticipated from the substrate HSFR value. The non-specular scattering measurements for each of the mirrors provide an

important verification of the surface PSD characterization and provide confidence in calculations of the flare of the assembled camera.

Mirror	M1	M2	M3	M4
Substrate HSFR (nm rms)	0.24	0.19	0.24	0.17
R_{\max} (%)	63.8	65.2	63.8	66.7
TIS (%)	4.3	2.9	3.1	1.4
Sum of R_{\max} and TIS (%)	68.1	68.1	66.9	68.1

Table 3: Measured high frequency roughness (HSFR) of the substrate, peak reflectivity (R_{\max}), and total integrated scattering (TIS) for the four ETS Set 2 camera mirrors. The sum of R_{\max} and TIS gives the mirror reflectance assuming an ideally smooth substrate.

CONCLUSIONS

The four ETS Set 2 projection mirrors have been successfully multilayer-coated and characterized by means of EUV reflectance and EUV scattering measurements. Outstanding levels of wavelength matching and thickness uniformity were achieved for all mirrors. Added figure errors due to the multilayer coatings were maintained well within the 0.11 nm rms specification. The measured results were implemented in calculations and it was verified that the Set 2 multilayer coatings will not contribute any aberrations in the printing of 70-nm dense features by the ETS camera.

ACKNOWLEDGEMENTS

The authors gratefully acknowledge Rick Levesque, Jay Ayers, George Wells, Todd Decker, Gary Heaton, Dave Mueller, Susan Ratti (LLNL) and Paul Denham, Dave Richardson and Stan Mrowka (LBNL), for their technical support of this work. We would like to thank Don Sweeney (LLNL) and Dave Attwood (LBNL) for many enlightening discussions.

This work was performed under the auspices of the U.S. Department of Energy by the University of California Lawrence Livermore National Laboratory under Contract No. W-7405-ENG-48. Funding was provided by the Extreme Ultraviolet Limited Liability Company (EUV LLC) under a Cooperative Research and Development Agreement (CRADA). The work performed at Lawrence Berkeley National Laboratory was supported through a CRADA with the EUV LLC and by the U.S. Department of Energy under contract No. DE-AC03-76F00098.

REFERENCES

1. R.H. Stulen and D.W. Sweeney, "Extreme Ultraviolet Lithography," IEEE J. Quantum Elec. **35**, 694-699 (1999).
2. C.W. Gwyn, R. Stulen, D. Sweeney, and D. Attwood, "Extreme ultraviolet lithography," J. Vac. Sci. Technol. B **16**, 3142-3149 (1998).
3. D. A. Tichenor, G. D. Kubiak, W. C. Replogle, L. E. Klebanoff, J. B. Wronosky, L. C. Hale, H. N. Chapman, J. S. Taylor, J. A. Folta, C. Montcalm, R. M. Hudyma, K. A. Goldberg, and P. Naulleau, "EUV Engineering Test Stand," *Emerging Lithographic Technologies IV*, E. A. Dobisz, Ed., Proceedings of SPIE Vol. 3997, 48-69 (2000).
4. D.A. Tichenor *et al.*, "System Integration and Performance of the EUV Engineering Test Stand," this Conference Proceedings.
5. C. Montcalm, R.F. Grabner, R.M. Hudyma, M.A. Schmidt, E. Spiller, C.C. Walton, M. Wedowski, and J. A. Folta, "Multilayer coated optics for an alpha-class extreme ultraviolet lithography system," in *EUV, X-Ray, and Neutron Optics and Sources*, S. P. Vernon and K. Goldberg, Eds., Proceedings of SPIE Vol. 3767, 210-216 (1999).
6. D.W. Sweeney, R.M. Hudyma, H.N. Chapman, D. Shafer, "EUV optical design for a 100 nm CD imaging system," in *Emerging Lithographic Technologies II*, Y. Vladimirski, Ed., Proceedings of SPIE Vol. 3331, 2-10 (1998).
7. J.H. Underwood, E.M. Gullikson, "High-resolution, high-flux, user friendly VLS beamline at the ALS for the 50-1300 eV energy region," J.Electr. Spectr. Rel. Phenom. **92**, 265-272 (1998).
8. E.M. Gullikson, S. Mrowka, B.B. Kaufmann, "Recent developments in EUV reflectometry at the Advanced Light Source," this Conference Proceedings.
9. V. Holy and T. Baumbach, "Non-specular x-ray reflection from rough multilayers," Phys. Rev. B **49**, 10668-76 (1994).
10. D.G. Stearns, "Stochastic model for thin film growth and erosion," Appl. Phys. Lett. **62**, 1745-7 (1993).